ce/papers Proceedings in civil engineering

Ernst & Sohn A Wiley Brand

ORIGINAL ARTICLE

eurosteel AMSTERDAM 2023

Ernst & Sohn A Wiley Brand

The effect of temperature actions on single-sided fillet welds in small-sized box girders of bridges

Malik Ltaief[1] | Martin Mensinger[1]

Correspondence

Malik Ltaief, M.Sc.

Technical University of Munich
Chair of Metal Structures
Arcisstrasse 21
80333 Munich
Germany
Email: m.ltaief@tum.de

[1] TUM, Munich, Germany

Abstract

The use of small-sized box girders has shown to bring numerous benefits in the design of bridges with short to medium spans. Therefore, it has become an established construction method in Germany. However, the beams are not accessible for inspection due to their small size, requiring the girder to be welded airtight. The limited accessibility also has consequences on the manufacturing process. Two of the four longitudinal fillet welds can only be executed from outside resulting in single-sided fillet welds. As a result of the airtight construction, temperature actions lead to fluctuation of the internal pressure of the box. The single-sided fillet welds are consequently subjected to unscheduled bending stress, which has an unclear impact on the weld. Subject of the research project, presented in this paper, is the influence of this unscheduled load case on the load-bearing capacity of the girder. To quantify the temperature which leads to changes of the internal pressure, numerical studies based on meteorological data are performed. The load-bearing behavior of single-sided fillet welds is investigated in experiments. It can be shown that the load-bearing capacity is underestimated by simplified calculation methods.

Keywords

steel bridges, small-sized hollow boxes, temperature loads, bending on single-sided fillet welds

1 Introduction

Small-sized hollow box girders are a widely used construction method for steel and composite bridges in Germany. This results from their wide variety of applications as well as structural and economic advantages. The advantages include high torsional stiffness of the girders, a high degree of prefabrication resulting in short installation times, and the possibility of waiving the internal corrosion protection layer.

Scheduled inspections inside the box girders are not possible due to the low construction height, which can be up to 1.20 m for small box girders. In order to prevent damage this method of construction demands a particularly high level of airtightness from the box girder.

Bridge structures are exposed to climatic conditions that vary daily and seasonally, resulting in alternating heating and cooling of the structure. This also causes temperature fluctuations inside the airtight welded hollow box, which lead to pressure variations due to the box's airtightness. These pressure variations are directly proportional to the temperature and can be described by the ideal gas law. Measurements on a composite bridge consisting of a three-web T-girder with airtight welded boxes [1] confirm that daily and seasonal pressure changes occur in such structures. By measuring the internal pressure over three years, a maximum pressure difference of 10 kN/m² could be measured on this structure [1]. These pressure fluctuations lead to an unscheduled load case of the bridge girder, as shown in Figure 1. The longitudinal welds, which are designed for longitudinal shear from traffic and dead loads, are now additionally subjected to this unscheduled

https://doi.org/10.1002/cepa.2547

load case.

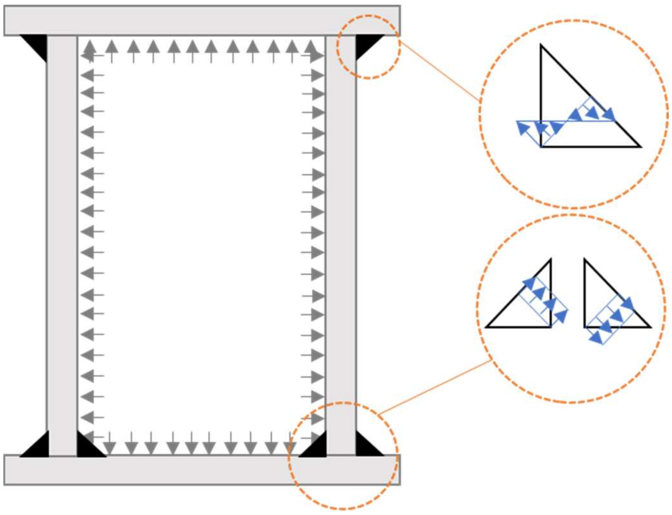

Figure 1 Internal pressure applying an additional bending load to the longitudinal fillet welds.

As a result of geometrical limitations, it is impossible to weld all four longitudinal fillet welds from both the inside and outside of the girder. As a result, only two longitudinal welds can be welded from the outside of the box, leading to single-sided fillet welds. In case of single-sided fillet welds, the bending moment resulting from the internal pressure cannot be carried by a pair of forces as in the case of the two-sided fillet welds, as shown in Figure 1. The welds are therefore subjected to a bending load. The design of single-sided fillet welds subjected to bending is only vaguely covered in the currently valid standard EN 1993-1-8 [2]. The design and execution of such welds in airtight closed box girders is part of a broad technical discussion. Within the research project "Economic dimensioning of fillet welds of tightly welded box girders" numerical and experimental investigations concerning the behavior and the load-bearing capacity of single-sided welded box girders will be carried out at the Technical University of Munich. To quantify the internal pressure loading, initial numerical investigations are conducted using weather data. The simulations span a period of 10 to 20 years. This allows the design value of the temperature to be extrapolated using the internal temperature based on the return period of the internal air temperature. Experimental investigations on single-sided fillet welds subjected to bending as well as combination of bending and shear loads can be used to determine the structural behavior of single-sided fillet welds. Furthermore, the structural behavior and load-bearing capacity of tightly welded box girders will be investigated by means of large-scale tests on box girders.

2 Numerical temperature investigations on air-tight welded box girders

2.1 Climatic actions on structures

Buildings are exposed to daily and seasonal variations in temperature. These variations depend on their location, orientation, and topographical conditions. Figure 2 shows the main climatic influences on a building. Particularly in the summer months, the global solar radiation, which can be divided into direct and diffuse radiation, causes the building to heat up. Direct solar radiation is characterized by shading, while diffuse radiation causes the building to heat up even on cloudy days. Depending on the reflection properties of the ground, the global solar radiation is reflected and affects the heat balance of the building, albeit to a lesser extent than the non-reflected radiation. In addition, the building interacts with the environment through longwave radiation. Essentially, this radiation exchange occurs between the ground and the building, as well as between the atmosphere and the building. At last, influenced by wind speed and air temperature, convective interaction takes place between the building and the surrounding air.

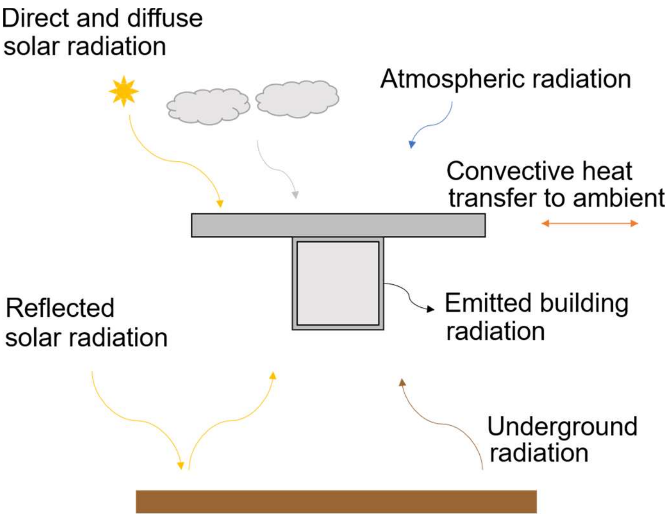

Figure 2 Main climatic effects on buildings.

The transient temperature state of the building can be described by collecting climate data such as radiation data, air temperature and wind speed. This data can be pre-processed and used for FE simulations. While constant weather station data is available, the approach of running simulations based on real data has a major advantage, allowing the complex weather phenomena to be considered, as well as specific boundary conditions. The time series of internal temperature can be used to statistically determine the design air temperature according to the code EN 1991-1-5 [3].

2.2 Numerical calculation of climatic action on bridges

In order to describe a non-stationary temperature field of a building, a thermal analysis is performed. Measured and processed weather data is used as climatic boundaries. The boundaries consist of a time series of measured data and should be continuously available over a period of several years. The processing of the weather data is carried out according to [4]. In a first step, the time series of the measured data are checked for completeness and accuracy. If necessary, measurement errors are closed and corrected.

The station 4928 - Stuttgart of the “German Weather Service” (DWD) [5, 6] is the source of the data used and presented in this paper. The weather data used from this station is available in a continuous time series over a time period from 2009 to 2022. From this database temperature, direct and diffuse radiation, and wind speed are assigned to the corresponding heat transfer process (Figure 3). The wind speed is calculated into a heat transfer coefficient according to [3] and [4], which is used in combination with the ambient air temperature for the numerical calculation of the convective heat transfer. Longwave radiation between the ground and the building as well as the atmosphere and the building are also modelled on base of the ambient air temperature. Since weather stations usually do not provide the ground temperature, the temperature of the ground is coupled with the ambient air temperature according to [2]. This coupling allows modelling the long wave interaction between the structure and the ground by calculating visibility factors and corresponding emission coefficients. In the same way, the atmospheric longwave radiation is coupled to the air temperature considering the corresponding view factors and emissivity values. The shortwave solar radiation is modeled using the measured shortwave solar heat flux data. The modelling considers the emission coefficients for shortwave radiation and visibility factors, as well as shading effects that depend on the position of the sun and the orientation of the bridge. The resulting heat flow is applied to the FE model as a heat flux across the building surfaces.

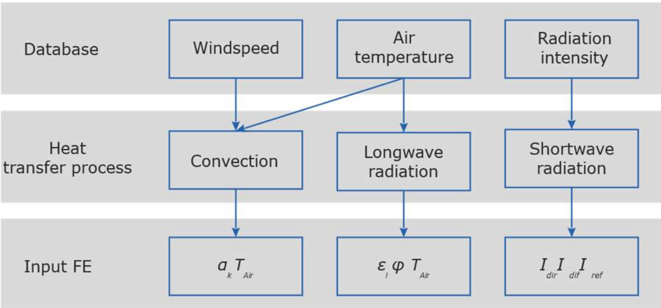

Figure 3 Data processing procedure.

The examined cross-section is a fictitious bridge cross-section (Figure 5). The section consists of a 20 cm thick concrete slab with a 40 cm cantilever. The steel box girder has a height of 80 cm and a width of 50 cm. The steel plates are 25 mm thick. The orientation of the cross-section is from north to south. The thermodynamic properties are summarized in Table 1, taken from [7]. The emission coefficients on the horizontal surface are chosen to be equal to those of a bituminous surface in order to consider the faster heating of a bituminous road surface. The heat transfer coefficient inside the box girder between the air and the surface is set at 4.5 W/m²K. DC2D4 elements were used for the thermal FE simulations. An edge length of 10 mm was used for meshing. The transient analysis has been carried out with a fixed step size of 20 minutes for each step.

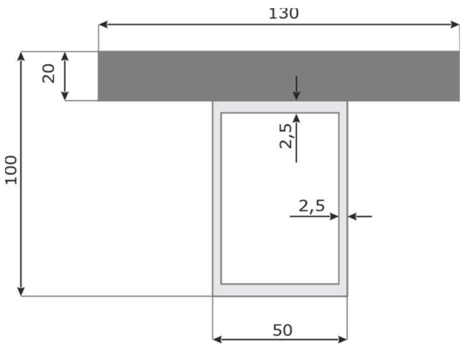

Figure 5 Geometry of the investigated cross-section.

Figure 4 (a) shows the nodal temperature where the sun is just above the horizon which leads to one-sided heating of the east-facing parts of the cross-section. The one-sided heating creates a horizontal temperature gradient within the structure. During midday hours (Figure 4(b)), the solar radiation only affects the road surface. A constant temperature curve is established horizontally. Since the temperature level of the building is now higher than the ambient temperature, the structure is only heated by the short-wave solar radiation. As the day progresses and the sun moves west, the cantilevers no longer provide shade, exposing the west-facing web of the structure to solar radiation (Figure 4 (c)). Similar to the morning hours, this

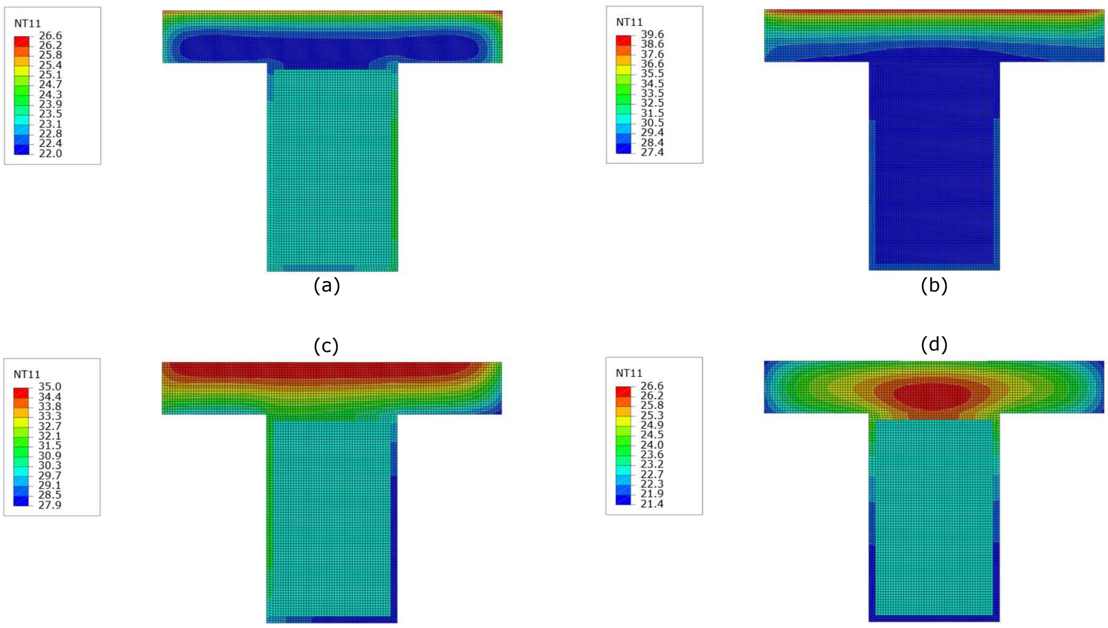

Figure 4 Simulation of the temperature field of the cross-section on a summer day at different times. (a) Morning hours, (b) Noon, (c) Evening, (d) Night.

creates a horizontal temperature gradient. At night, convective heat transfer and long-wave radiation from the bridge to the ambient cause the cross-section to cool down (Figure 4 (d)). Due to thermal inertia, the concrete cross-section cools down slower than the rest of the cross-section and stores heat. In the following days, heating occurs in a similar manner depending on the climatic boundary conditions.

Table 1 Material properties.

Material	ρ (kg/m³)	c_p (J/kgK)	λ (W/mK)	ϵ_{short}	ϵ_{long}
Steel	7840	460	46	0,7	0,6
Concrete	2400	960	2.1	0,7	0,9
Air	1,25	1000	100	-	-
Bitumen	-	-	-	0,88	0,9

3 Statistical evaluation of the simulated internal air temperature

According to code EN 1991-1-5 [3], the characteristic value for temperature loads is defined as the statistical mean of reaching or exceeding the temperature once in every 50 years. This corresponds to the temperature that is exceeded with a probability of 98%. In order to determine the exceedance temperature, the temperature data must be approximated to a distribution function. The 13-year time series obtained from chapter 2 (Figure 6) is processed according to extreme value statistics. The assumption that the temperature data under investigation are independent and identically distributed is a prerequisite for the application of the statistical methods. To obtain independent temperature samples, the time series is divided into blocks of a length of one year. From these, the maximum temperature is extracted to obtain 17 independent samples of the internal air temperature (Figure 6).

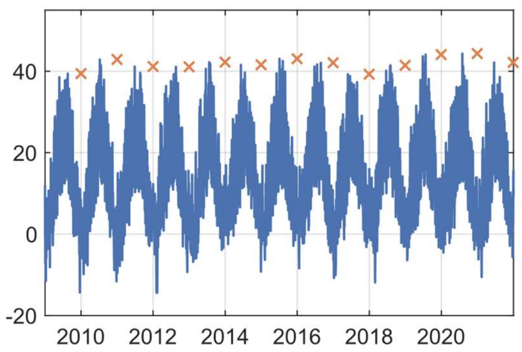

Figure 6 Results of the simulation of the internal air temperature and annual maximum values.

Based on [8] and [9], the maximum values of the blocks can be approximated to one of the existing extreme value distributions. The parameters of the distribution function can be determined using a maximum likelihood estimator. In this case the samples are approximated to the general extreme value distribution. The estimated parameters are shown in Table 2 with the corresponding standard deviation.

Table 2 Parameters of the generalized extreme value distribution.

Parameter	Expected value	Standard deviation
Shape parameter k	-0.422	0.24
Scale parameter σ	1.542	0.36
Location parameter μ	41.50	0.48

By forming the inverse cumulative distribution function, the return period of different temperature levels can be determined. Figure 7 shows the return period. The characteristic value for the internal temperature load can be read on a return period of 50 years and is found to be at 44.5°C.

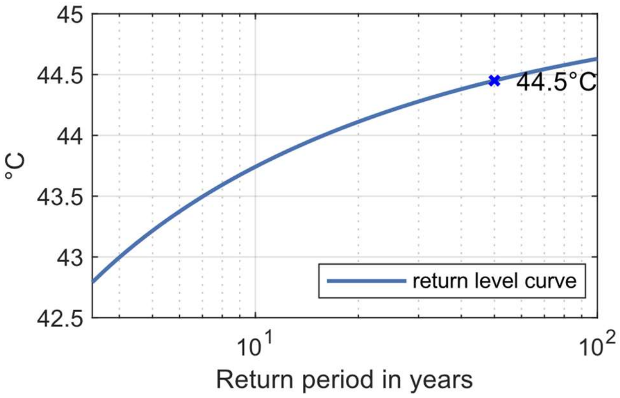

Figure 7 Return level curve of the internal temperature based on thermal simulations.

In order to determine the internal pressure, it is necessary to know the sealing temperature. In Germany, the average mounting temperature is 10°C [10]. Assuming that the hollow section is hermetically sealed at an average atmospheric pressure of 1013.2 hPa and at the mounting temperature, the design values for the internal pressure can be determined using the ideal gas law (eq. 6).

$$p_{internal} = p_0 \cdot \frac{\theta_{internal}}{\theta_0} - p_0 \quad (6)$$

The characteristic value of the internal pressure can be determined from these assumptions and is found to be 12.3 kN/m².

4 Experimental investigations on single-sided fillet welds

The small size of the box girder makes it impractical to weld all longitudinal fillet welds from both sides, which was outlined in the introduction. According to section (4.12) of EN 1993-1-8: 2010 [2], fillet welds should not be subjected to bending stress. One way to avoid bending stress in single-sided fillet welds is executing the welds as

bevel-groove weld. However, from an economic point of view, this has a negative impact on the weld due to the seam preparation and additional work in the weld.
To evaluate the load-bearing capacity of single-sided fillet welds regarding bending stress, experimental investigations on their load-bearing behavior are being conducted at the Technical University of Munich. Initial results indicate that the load-bearing capacity is higher than expected based on simplified calculations.

4.1 Experimental set-up

Two 20 mm thick plates were welded together with a 5 mm single-sided fillet weld. The specimens are fixed to a clamping fixture. A load is applied to the weld at a distance of 140 mm by using a hydraulic press (Zwick 600) to introduce a bending moment into the weld (Figure 8). The material parameters of the specimen and the weld are summarized in the following Table 3.

Table 3 Specimen parameters

Specimen no.	Steel grade	Filler material
1 - 3	S355	T46 3M

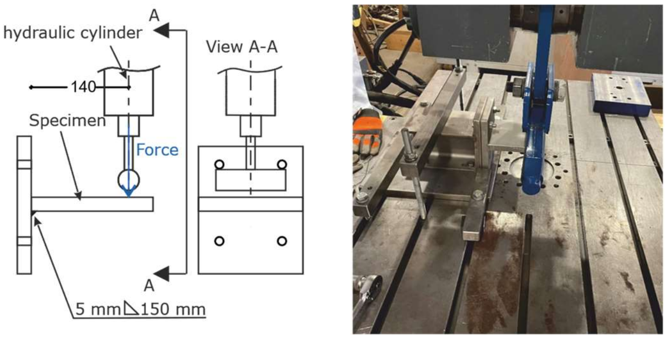

Figure 8 Experimental set-up.

The tests were carried out under displacement control. The weld was tested to failure. Force and corresponding rotation were recorded. In addition, digital image correlation (DIC) measurements were taken to evaluate the strain distribution in the welding.

4.2 Test results

The following Figure 9 shows the moment-rotation behavior for the tests carried out. Note that the bending capacity is normalized to the weld length. It is evident that the maximum load capacity of the weld is reached at approximately 2 degrees.

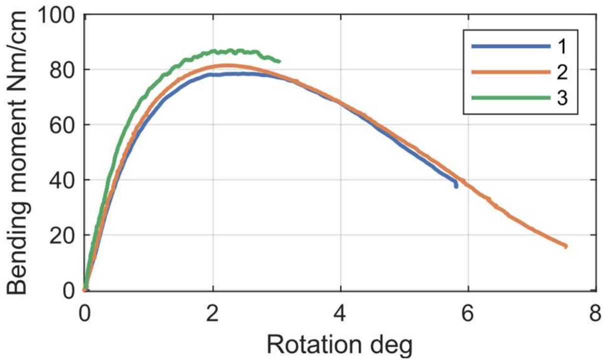

Figure 9 Moment rotation behaviour of the fillet welds.

The angle was calculated from the DIC measurements. Figure 10 shows two DIC images before the weld was loaded (a) and when the weld was loaded to 86 Nm/cm (b).

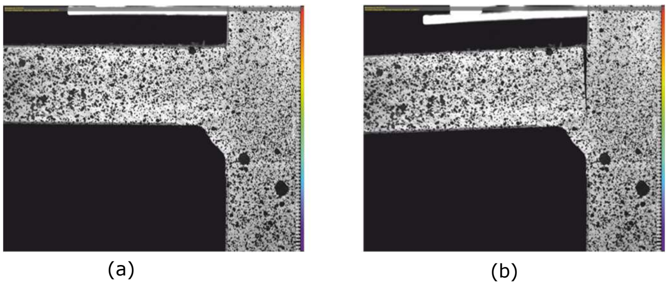

Figure 10 Image sequence from DIC, (a) without load, (b) under a load of 86 Nm/cm.

In order to compare the maximum experimental strength obtained with the theoretical strength of the weld, the bending resistance of the fillet weld is calculated. In a first step, the effective thickness of the weld has to be determined to take into account the deeper fused face. For this purpose, the specimens were cut and embedded in epoxy resin. They were ground, polished and etched with Nital. The weld thickness was measured using a Leica DM4 B light microscope. Knowing the effective weld thickness, the elastic and plastic modulus can be calculated from the weld thickness and weld length using equations (1) and (2).

$$W_{el} = \mathrm{a}_{\mathrm{w}}^2 \cdot \frac{l_w}{6} \qquad (1)$$

$$W_{pl} = \mathrm{a}_{\mathrm{w}}^2 \cdot \frac{l_w}{4} \qquad (2)$$

The normal stress is limited in EN 1993-1-8 [2] section (4.5.3) by taking into account the tensile strength using the following equation:

$$\sigma_{\perp} \leq 0{,}9 \cdot \frac{\mathrm{f_u}}{\gamma_{\mathrm{M2}}} \qquad (3)$$

By substituting equation (1) or (2) in

$$\sigma_{\perp} = \frac{M}{W} \qquad (4)$$

and using equation (3) the bending strength of the weld can be calculated in a simplified manner:

$$M_R = \frac{0{,}9 \cdot f_u}{\gamma_{M2}} \cdot W \qquad (5)$$

Table 4 compares the calculated elastic and plastic resistance to the effective resistance as a function of weld thickness for specimens 1 to 3. For comparability, the partial safety factor γ_{M2} is chosen to be 1.0. The tensile strength of S355 steel is 490MPa.

Table 4 Comparison between the calculated and experimental load-bearing capacity

<table>
<tr><th>Specimen no.</th><th>Experimental (Nm/cm)</th><th>a_w (mm)</th><th>Elastic (Nm/cm)</th><th>Plastic (Nm/cm)</th></tr>
<tr><td>1</td><td>80.3</td><td rowspan="2">5.5</td><td rowspan="2">22.2</td><td rowspan="2">33.3</td></tr>
<tr><td>2</td><td>81.5</td></tr>
<tr><td>3</td><td>88.8</td><td>5.9</td><td>24.7</td><td>37.0</td></tr>
</table>

Table 4 shows that the effective load-bearing capacity is higher than the calculated load-bearing capacity. This is attributed to higher material strength in the weld. It is also suspected that the stress distribution will not ideally distribute across the weld thickness as assumed in the simplified calculation model. Ongoing investigations are expected to provide further insights into his matter.

5 Conclusion and outlook

Using numerical simulations, it was possible to show that airtight welded small-sized box girders are exposed to additional internal pressure due to external temperature effects. For this purpose, a numerical model based on weather data was developed. This model was used to generate a time series of the internal air temperature. The time series has been analyzed by means of extreme value statistics. By extrapolating the generated temperature data, the characteristic value of the internal air and consequently the internal pressure could be determined. Bending tests were conducted on single-sided fillet welds to investigate their load-bearing capacity and rotational behavior. The results showed that the welds had a higher load-bearing capacity than the calculations predicted. The question arises whether the design of single-sided fillet welds subjected to bending stresses should be included in the standards. This could be clarified by extensive numerical and experimental investigations. Longitudinal fillet welds of box girders are subjected to longitudinal shear stress caused by traffic and dead weight loads. For that reason, the load-bearing capacity of the single-sided fillet welds should be investigated under a combinate longitudinal share and bending. Additionally, large-scale tests have to be conducted to consider the overall load-behavior of the box girder. Based on the observed rotational capacity of the welds, these tests aim to investigate whether the rotational capacity leads to a redistribution of the bending moment into the plates.

6 Acknowledgement

The research project IGF "Economic dimensioning of fillet welds of tightly welded box girders", IGF-Project no. 22244 from the Research Association "German Committee for Steel Construction" (DASt), Sohnstraße 65, 40237 Düsseldorf, is supported by the Federal Ministry of Economic Affairs and Climate Action the German Federation of Industrial Research Associations (AiF) as part of the programme for promoting industrial cooperative research (IGF) on the basis of a decision by the German Bundestag.

References

[1] Radtke, F.; Schubart R. (2019) *Contribution to the design approach of welds in air-tight box girders under temperature induced internal pressure*. Stahlbau 88, vol. 12

[2] EN 1993-1-8 (2005) *Eurocode 3: Design of steel structures - Part 1-8: Design of joints*

[3] EN 1991-1-5 (2003) *Eurocode 1: Actions on structures - Part 1-5: General actions; Thermal actions*.

[4] Mangerig, I. (1986) *Klimatische Temperaturbeanspruchung von Stahl- und Stahlverbundbrücken.* Bochum

[5] DWD Climate Data Center (CDC) (2022): *Historical 10-minute station observations of solar incoming radiation, longwave downward radiation and sunshine duration for Germany*. version V1

[6] DWD Climate Data Center (CDC) (2022): Historical 10-minute station observations of mean wind speed and wind direction for Germany. version V1

[7] Lichte, U. (2005) *Klimatische Temperatureinwirkungen und Kombinationsregeln bei Brückenbauwerken. München:* Berichte aus dem Konstruktiven Ingenieurbau, Universität der Bundeswehr München

[8] Coles, S. (2001) *An Introduction to Statistical Modeling of Extreme Values.* London: Springer

[9] McNeil, A.J.; Frey, R.; Embrechts, P. (2015) *Quantitative risk management.* Oxford: Princeton University Press

[10] Geißler, K. (2014) Handbuch Brückenbau. Berlin: Ernst & Sohn